

# Absorbing-state phase transitions on percolating lattices

Man Young Lee

*Department of Physics, Missouri University of Science and Technology, Rolla, MO 65409, USA*

Thomas Vojta

*Department of Physics, Missouri University of Science and Technology, Rolla, MO 65409, USA and  
Max-Planck-Institute for Physics of Complex Systems, Noethnitzer Str. 38, 01187 Dresden, Germany*

(Dated: June 21, 2024)

We study nonequilibrium phase transitions of reaction-diffusion systems defined on randomly diluted lattices, focusing on the transition across the lattice percolation threshold. To develop a theory for this transition, we combine classical percolation theory with the properties of the supercritical nonequilibrium system on a finite-size cluster. In the case of the contact process, the interplay between geometric criticality due to percolation and dynamical fluctuations of the nonequilibrium system leads to a new universality class. The critical point is characterized by ultraslow activated dynamical scaling and accompanied by strong Griffiths singularities. To confirm the universality of this exotic scaling scenario we also study the generalized contact process with several (symmetric) absorbing states, and we support our theory by extensive Monte-Carlo simulations.

PACS numbers: 05.70.Ln, 64.60.Ht, 02.50.Ey

## I. INTRODUCTION

In recent years, considerable effort has been directed towards identifying and classifying phase transitions far from thermal equilibrium. Such nonequilibrium transitions can be found in a wide variety of problems in biology, chemistry, and physics. Examples include population dynamics, the spreading of epidemics, surface chemical reactions, catalysis, granular flow, traffic jams as well as growing surfaces and interfaces (see, e.g., [1, 2, 3, 4, 5, 6, 7, 8]). Nonequilibrium phase transitions are characterized by large scale fluctuations and collective behavior in space and time very similar to the behavior at equilibrium critical points.

A particularly interesting situation arises when an equilibrium or nonequilibrium many-particle system is defined on a randomly diluted lattice. Then, two distinct types of fluctuations are combined, *viz.* the dynamical fluctuations of the many-particle system and the static geometric fluctuations due to lattice percolation [9]. In equilibrium systems, their interplay gives rise to novel universality classes for the thermal [10, 11, 12] and quantum [13, 14, 15, 16] phase transitions across the lattice percolation threshold.

In this paper, we investigate the interplay between dynamical fluctuations and geometric criticality in nonequilibrium many-particle systems. We focus on a particularly well-studied type of transitions, the so-called absorbing state transitions, that separate active, fluctuating steady states from inactive (absorbing) states in which fluctuations cease completely. The generic universality class for absorbing state transitions is directed percolation (DP) [17]. It is conjectured [18, 19] to be valid for all absorbing state transitions with scalar order parameter and no extra symmetries or conservation laws. In the presence of symmetries and/or conservation laws, other universality classes can be realized, such as the  $DP_n$  class

in systems with  $n$  symmetric absorbing states [20].

For definiteness, we consider the contact process [21], a prototypical system in the DP universality class. We show that the contact process on a randomly site or bond diluted lattice has two different nonequilibrium phase transitions: (i) a generic disordered DP transition at weak dilutions (below the lattice percolation threshold) driven by the dynamic fluctuations of the contact process and (ii) the transition across the lattice percolation threshold driven by the geometric criticality of the lattice. The former transition has been investigated for a number of years [22, 23, 24, 25]; it has recently retracted considerable attention because it is governed by an exotic infinite-randomness fixed point [26, 27, 28, 29]. In contrast, the latter transition has received much less attention.

Here, we develop a theory for the nonequilibrium transition across the lattice percolation threshold by combining classical percolation theory with the properties of the supercritical contact process on a finite-size cluster. We show that the critical point is characterized by ultraslow activated (exponential) dynamical scaling and accompanied by strong Griffiths singularities. The scaling scenario is qualitatively similar to the generic disordered DP transition, but with different critical exponent values. To confirm the universality of this exotic scenario, we also investigate the generalized contact process with  $n$  (symmetric) absorbing states [20]. This is a particularly interesting problem because the generic transition of the disordered generalized contact process does *not* appear to be of infinite-randomness type [26, 27].

The paper is organized as follows. In Sec. II, we introduce our models, the simple and generalized contact processes on a randomly diluted lattice. We also discuss the phase diagrams. In Sec. III we briefly summarize the results of classical percolation theory to the extent necessary for our purposes. Section IV contains the main

part of the paper, the theory of the nonequilibrium transition across the lattice percolation threshold. Section V is devoted to the question of the generality of the arising scaling scenario. We conclude in Sec. VI. A short account of part of this work has already been published in Ref. [30].

## II. SIMPLE AND GENERALIZED CONTACT PROCESSES ON DILUTED LATTICES

### A. Contact process

The clean contact process [21] is a prototypical system in the DP universality class. It is defined on a  $d$ -dimensional hypercubic lattice. (We consider  $d \geq 2$  since we will be interested in diluting the lattice.) Each lattice site  $\mathbf{r}$  can be active (infected, state A) or inactive (healthy, state I). During the time evolution of the contact process which is a continuous-time Markov process, each active site becomes inactive at a rate  $\mu$  (“healing”) while each inactive site becomes active at a rate  $\lambda m/(2d)$  where  $m$  is the number of active nearest neighbor sites (“infection”). The infection rate  $\lambda$  and the healing rate  $\mu$  are external parameters. Their ratio controls the behavior of the contact process.

For  $\lambda \ll \mu$ , healing dominates over infection, and the absorbing state without any active sites is the only steady state of the system (inactive phase). For sufficiently large infection rate  $\lambda$ , there is a steady state with a nonzero density of active sites (active phase). These two phases are separated by a nonequilibrium phase transition in the DP universality class at a critical value  $(\lambda/\mu)_c^0$  of the ratio of the infection and healing rates.

The basic observable in the contact process is the average density of active sites at time  $t$ ,

$$\rho(t) = \frac{1}{L^d} \sum_{\mathbf{r}} \langle n_{\mathbf{r}}(t) \rangle \quad (1)$$

where  $n_{\mathbf{r}}(t) = 1$  if the site  $\mathbf{r}$  is active at time  $t$  and  $n_{\mathbf{r}}(t) = 0$  if it is inactive.  $L$  is the linear system size, and  $\langle \dots \rangle$  denotes the average over all realizations of the Markov process. The longtime limit of this density (i.e., the steady state density)

$$\rho_{\text{stat}} = \lim_{t \rightarrow \infty} \rho(t) \quad (2)$$

is the order parameter of the nonequilibrium phase transition.

### B. Generalized contact process

Following Hinrichsen [20], we now generalize the contact process by introducing  $n$  different inactive states  $I_k$  with  $k = 1 \dots n$  ( $n = 1$  corresponds to the simple contact process). Here,  $k$  is sometimes called the “color” label.

The time evolution is again a continuous-time Markov process. The first two rates are equivalent to those of the simple contact process: An active site can decay into each of the inactive states  $I_k$  with rate  $\mu/n$ , and a site in any of the inactive states becomes active at a rate  $\lambda m/(2d)$  with  $m$  the number of active nearest-neighbor sites. To introduce competition between the different inactive states, we define a third rate: If two neighboring sites are in *different* inactive states, each can become active with a rate  $\sigma$ . This last rule prevents the boundaries between domains of different inactive states from sticking together infinitely. Instead they can separate, leaving active sites behind.

The properties of the clean generalized contact process have been studied in some detail in the literature [20, 31]. If the boundary activation rate  $\sigma$  vanishes, the behavior becomes identical to the simple contact process for all  $n$ . (This becomes obvious by simply dropping the color label and treating all inactive sites as identical.) For  $\sigma > 0$ , the system becomes “more active” than the simple contact process, and the universality class changes. In one space dimension, a phase transition exists for  $n = 1$  (in the DP universality class) and for  $n = 2$  (in the  $Z_2$ -symmetric directed percolation (DP2) class which coincides with the parity-conserving (PC) class in one dimension [5]). For  $n \geq 3$  the system is always in the active phase, and no phase transition exists at finite values of  $\lambda$ ,  $\mu$  and  $\sigma$ .

The generalized contact process in higher space dimensions presumably behaves in an analogous fashion: There is a DP transition for  $n = 1$  while the properties for  $n > 1$  are different. For sufficiently large  $n$ , the system is always active [32].

### C. Lattice dilution

We now introduce quenched site dilution by randomly removing each lattice site with probability  $p$ . (Bond dilution could be introduced analogously.) As long as the vacancy concentration  $p$  remains below the lattice percolation threshold  $p_c$ , the lattice consists of an infinite connected cluster of sites accompanied by a spectrum of finite-size clusters. In contrast, at dilutions above  $p_c$ , the lattice consists of disconnected finite-size clusters only.

Figure 1 schematically shows the resulting phase diagrams of the nonequilibrium process as a function of the infection rate  $\lambda$  and dilution  $p$ , keeping the healing rate  $\mu$  and the boundary activation rate  $\sigma$ , if any, constant. Depending on the properties of the clean undiluted system, there are two qualitatively different cases.

(a) If the undiluted system has a phase transition at a nonzero critical infection rate  $\lambda_c^0$ , the active phase survives for all vacancy concentrations below the percolation threshold,  $p < p_c$ . It even survives at the percolation threshold  $p_c$  on the critical percolation cluster because it is connected, infinitely extended, and its fractal dimension  $D_f$  is larger than unity. The critical infection rate  $\lambda_c$  increases with increasing dilution  $p$  to compensate for the

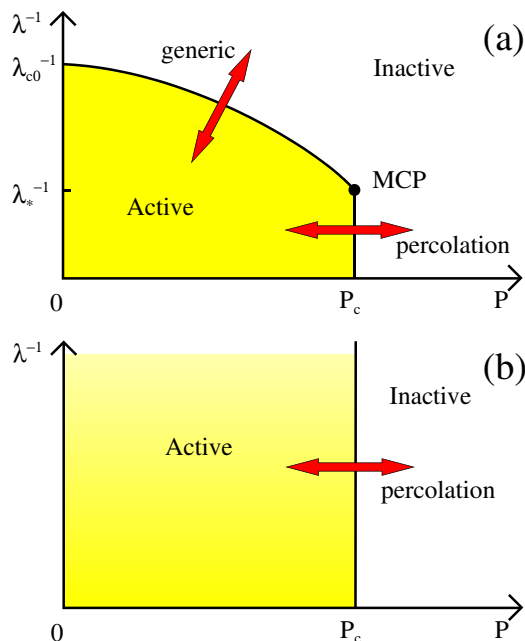


FIG. 1: (Color online:) Schematic phase diagrams for the simple and generalized contact processes on a diluted lattice in dimensions  $d \geq 2$  as a function of dilution  $p$  and inverse infection rate  $\lambda^{-1}$  (healing and boundary activation rates  $\mu$  and  $\sigma$  are fixed). Case (a) applies to systems that display a phase transition at  $\lambda_c^0$  in the absence of dilution. There is a multicritical point (MCP) at  $(p_c, \lambda_*)$  separating the generic transition from the lattice percolation transition. Case (b) is for systems that are always active in the absence of dilution.

missing neighbors, reaching  $\lambda_*$  at  $p_c$ . The active phase cannot exist for  $p > p_c$  because the lattice consists of finite-size clusters only, and the nonequilibrium process will eventually end up in one of the absorbing states on any finite-size cluster. Thus, in case (a), our system features two nonequilibrium phase transitions, (i) a generic (disordered) transition for dilutions  $p < p_c$ , driven by the dynamic fluctuations of the nonequilibrium process and (ii) the transition across the lattice percolation threshold driven by the geometric criticality of the lattice. They are separated by a multicritical point at  $(p_c, \lambda_*)$ .

(b) If the undiluted system is always active (as for the generalized contact process with a sufficiently high number of inactive states), the phase diagram is simpler. The active phase covers the entire region  $p \leq p_c$  for all  $\lambda > 0$  ( $\lambda_*$  is formally zero) while the inactive phase exists in the region  $p > p_c$ . There is no generic (disordered) nonequilibrium phase transition, only the transition across the lattice percolation threshold.

The focus of the present paper is the nonequilibrium phase transition across the lattice percolation threshold that exists in both cases. In order to develop a theory for this transition, we combine classical percolation theory with the properties of the nonequilibrium process on a finite-size cluster. In the next section we therefore briefly summarize key results of percolation theory.

### III. CLASSICAL PERCOLATION THEORY

Consider a regular lattice in  $d$  dimensions. If each lattice site is removed with probability  $p$  [33], an obvious question is whether or not the lattice is still connected in the sense that there is a cluster of connected (nearest neighbor) sites that spans the entire system. This question defines the percolation problem (see Ref. [9] for an introduction).

In the thermodynamic limit of infinite system volume, there is a sharp boundary between the cases of a connected or disconnected lattice. If the vacancy concentration  $p$  stays below the percolation threshold  $p_c$ , an infinite cluster of connected sites exists (with a probability of unity). For  $p > p_c$ , an infinite cluster does not exist, instead, the lattice consists of many disconnected finite-size clusters.

The behavior of the lattice for vacancy concentrations close to the percolation threshold can be understood as a (geometric) continuous phase transition or critical phenomenon. The order parameter is the probability  $P_\infty$  of a site to belong to the infinite connected percolation cluster. It is obviously zero in the disconnected phase ( $p > p_c$ ) and nonzero in the percolating phase ( $p < p_c$ ). Close to  $p_c$  it varies as

$$P_\infty \sim |p - p_c|^{\beta_c} \quad (p < p_c) \quad (3)$$

where  $\beta_c$  is the order parameter critical exponent of classical percolation. Note that we use a subscript  $c$  to distinguish quantities associated with the classical lattice percolation problem from those of the nonequilibrium phase transitions discussed later. In addition to the infinite cluster, we also need to characterize the finite clusters on both sides of the transition. Their typical size, the correlation or connectedness length  $\xi_c$  diverges as

$$\xi_c \sim |p - p_c|^{-\nu_c} \quad (4)$$

with  $\nu_c$  the correlation length exponent. The average mass  $S_c$  (number of sites) of a finite cluster diverges with the susceptibility exponent  $\gamma_c$  according to

$$S_c \sim |p - p_c|^{-\gamma_c} . \quad (5)$$

The complete information about the percolation critical behavior is contained in the cluster size distribution  $n_s$ , i.e., the number of clusters with  $s$  sites excluding the infinite cluster (normalized by the total number of lattice sites). Close to the percolation threshold, it obeys the scaling form

$$n_s(\Delta) = s^{-\tau_c} f(\Delta s^{\sigma_c}) . \quad (6)$$

Here  $\Delta = p - p_c$ , and  $\tau_c$  and  $\sigma_c$  are critical exponents. The scaling function  $f(x)$  is analytic for small  $x$  and has a single maximum at some  $x_{\max} > 0$ . For large  $|x|$ , it drops off rapidly

$$f(x) \sim \exp[-B_1 x^{1/\sigma_c}] \quad (x > 0), \quad (7)$$

$$f(x) \sim \exp\left[-\left(B_2 x^{1/\sigma_c}\right)^{1-1/d}\right] \quad (x < 0), \quad (8)$$

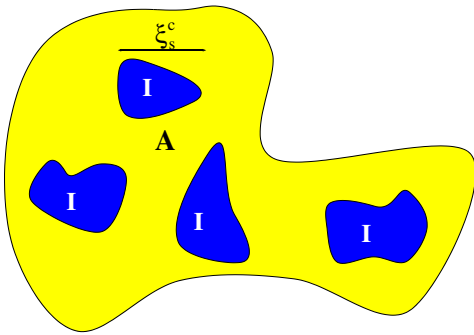


FIG. 2: (Color online:) Schematic of the metastable state of the supercritical contact process on a single percolation cluster. A and I denote active and inactive sites, and  $\xi_s^c$  is the connected correlation length of the density fluctuations on the cluster.

where  $B_1$  and  $B_2$  are constants of order unity. All classical percolation exponents are determined by  $\tau_c$  and  $\sigma_c$  including the correlation lengths exponent  $\nu_c = (\tau_c - 1)/(d\sigma_c)$ , the order parameter exponent  $\beta_c = (\tau_c - 2)/\sigma_c$ , and the susceptibility exponent  $\gamma_c = (3 - \tau_c)/\sigma_c$ .

Right at the percolation threshold, the cluster size distribution does not contain a characteristic scale. The structure of the critical percolation cluster is thus fractal with the fractal dimension being given by  $D_f = d/(\tau_c - 1)$ .

#### IV. NONEQUILIBRIUM TRANSITION ACROSS THE LATTICE PERCOLATION THRESHOLD

##### A. Single-cluster dynamics

To develop a theory of the nonequilibrium phase transition across the lattice percolation threshold, we first study the nonequilibrium process on a single connected finite-size cluster of  $s$  sites. For definiteness, this section focuses on the simple contact process. The generalized contact process will be considered in Sec. V.

The crucial observation is that on the percolation transition line (for  $\lambda > \lambda_*$ ), the contact process is supercritical, i.e., the cluster is locally in the active phase. The time evolution of such a cluster, starting from a fully active lattice, therefore proceeds in two stages: Initially, the density  $\rho_s$  of active sites decays rapidly towards a metastable state (which corresponds to the steady state of the equivalent *infinite* system) with a nonzero density of active sites and islands of the inactive phase of linear size  $\xi_s^c$  (see Fig. 2). This metastable state can then decay into the inactive (absorbing) state only via a rare collective fluctuation involving *all* sites of the cluster. We thus expect the long-time decay of the density to be of exponential form (suppressing subleading pre-exponential factors),

$$\rho_s(t) \sim \exp[-t/t_s(s)], \quad (9)$$

with a long lifetime  $t_s$  that increases exponentially with the cluster size  $s$

$$t_s(s) = t_0 \exp[A(\lambda)s] \quad (10)$$

for sufficiently large  $s$ . Here,  $t_0$  is some microscopic time scale.

The lifetime increases the faster with  $s$  the further the cluster is in the active phase. This means, the prefactor  $A(\lambda)$  which plays the role of an inverse correlation volume vanishes at the multicritical value  $\lambda_*$  and monotonically increases with increasing  $\lambda$ . Close to the multicritical point, the behavior of  $A(\lambda)$  can be inferred from scaling. Since  $A(\lambda)$  has the dimension of an inverse volume, it varies as

$$A(\lambda) \sim (\lambda - \lambda_*)^{\nu_* D_f} \quad (11)$$

where  $\nu_*$  is the correlation length exponent of the multicritical point and  $D_f$  is the (fractal) space dimensionality of the underlying cluster.

Note that (10) establishes an exponential relation between length and time scales at the transition. Because the number of sites  $s$  of a percolation cluster is related to its linear size  $R_s$  via  $s \sim R_s^{D_f}$ , eq. (10) implies

$$\ln t_s \sim R_s^{D_f}. \quad (12)$$

Thus, the dynamical scaling is activated rather than power-law with the tunneling exponent being identical to the fractal dimension of the critical percolation cluster,  $\psi = D_f$ .

To confirm the above phenomenological arguments, we have performed extensive Monte-Carlo simulations of the contact process on finite-size clusters using clean one-dimensional and two-dimensional systems as well as diluted lattices. Our simulation method is based on the algorithm by Dickman [34] and described in detail in Refs. [28, 29].

A characteristic set of results is shown in Fig. 3. It shows the time evolution of the contact process on several one-dimensional clusters of different size  $s$ , starting from a fully active lattice. The infection rate  $\lambda = 3.8$  (we set  $\mu = 1$ ) puts the clusters (locally) in the ordered phase, i.e., it is supercritical, since the critical value in one dimension is  $\lambda_c = 3.298$ . All data are averages over  $10^5$  independent trials. The double-logarithmic plot of density  $\rho_s$  vs. time  $t$  in Fig. 3a clearly shows the two-stage time evolution consisting of a rapid initial decay (independent of cluster size) towards a metastable state followed by a long-time decay towards the absorbing state which becomes slower with increasing cluster size. Replotting the data in log-linear form in Fig. 3b confirms that the long-time decay is exponential, as predicted in (9).

The lifetime  $t_s$  of the contact process on the cluster can be determined by fitting the asymptotic part of the  $\rho_s(t)$  curve to (9). Figure 4 shows the lifetime as a function of cluster size  $s$  for four different values of the infection

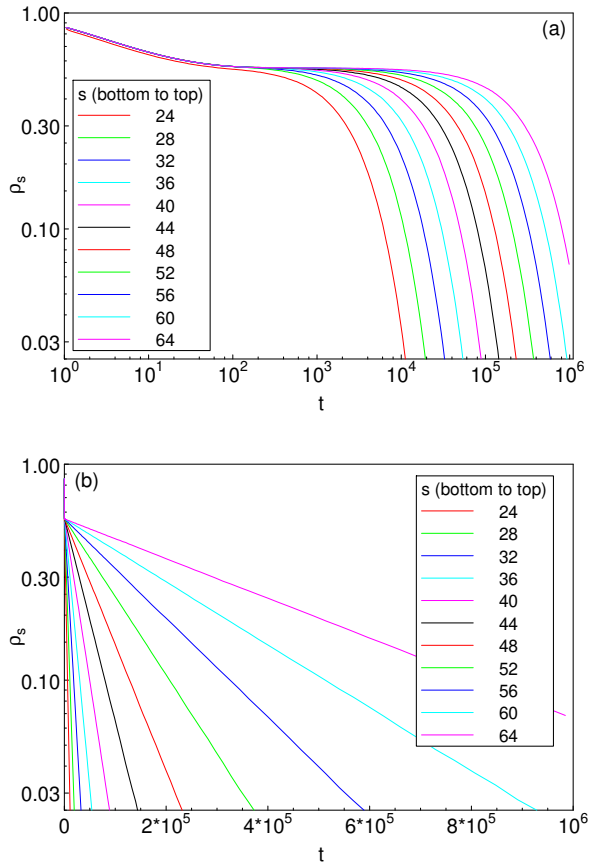


FIG. 3: (Color online:) Contact process on one-dimensional clusters of size  $s$ , starting from a fully active lattice at  $\lambda = 3.8$ ,  $\mu = 1$  which is in the active phase. (a) Double-logarithmic plot of density vs. time showing the two-stage time-evolution via a metastable state. (b) Log-linear plot demonstrating that the long-time decay is exponential. All data are averages over  $10^5$  independent runs.

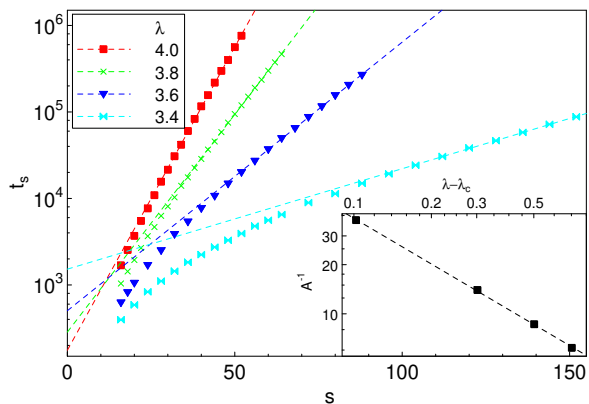


FIG. 4: (Color online:) Lifetime  $t_s$  as a function of cluster size  $s$  for different values of the infection rate  $\lambda$ . The other parameters are as in Fig. 3. The dashed lines are fits of the large- $s$  behavior to the exponential dependence (10). Inset: Correlation volume  $A^{-1}$  as a function of the distance from bulk criticality. The dashed line is a power-law fit.

rate  $\lambda$ . Clearly, for sufficiently large clusters, the lifetime depends exponentially on the cluster size, as predicted in (10). (The data for  $\lambda = 3.4$  which is very close to the bulk critical point of  $\lambda_c = 3.298$  have not fully reached the asymptotic regime as can be seen from the remaining slight curvature of the plot.) By fitting the large- $s$  behavior of the lifetime curves to the exponential law (10), we obtain an estimate of the inverse correlation volume  $A$ . The inset of Fig. 4 shows this correlation volume as a function of the distance from the bulk critical point. In accordance with (11) it behaves as a power law. The exponent value of approximately 0.95 is in reasonable agreement with the prediction  $\nu = 1.097$  for our one-dimensional clusters.

We have performed analogous simulations for various sets of two-dimensional clusters as well as finite-size diluted lattices. In all cases, the Monte-Carlo results confirm the phenomenological theory summarized in eqs. (9), (10), and (11).

### B. Steady-state density and density decay

We now consider the full problem, the contact process on a diluted lattice close to the percolation threshold. To obtain observables of the entire system, we must sum over all percolation clusters.

Let us start by analyzing static quantities such as the steady state density  $\rho_{st}$  of active sites (the order parameter of the nonequilibrium transition) and the spatial correlation length  $\xi_{\perp}$ . Finite-size percolation clusters do not contribute to the steady-state density because the contact process eventually decays into the absorbing inactive state on any finite-size cluster. A steady-state density can thus exist only on the infinite percolation cluster for  $p < p_c$ . For  $\lambda > \lambda_*$ , the infinite cluster is supercritical, i.e., a finite fraction of its sites is active. Thus, the total steady-state density is proportional to the number of sites in the infinite cluster,

$$\rho_{st} \sim P_{\infty}(p) \sim \begin{cases} |p - p_c|^{\beta_c} & (p < p_c) \\ 0 & (p > p_c) \end{cases}. \quad (13)$$

Consequently, the order parameter exponent  $\beta$  of the nonequilibrium transition is identical to the corresponding exponent  $\beta_c$  of the lattice percolation problem.

The (average) spatial correlation length  $\xi_{\perp}$  of the nonequilibrium process can be found using a similar argument. On the one hand, the spatial correlations of the contact process cannot extend beyond the connectedness length  $\xi_c$  of the underlying diluted lattice because different percolation clusters are completely decoupled. This implies  $\xi_{\perp} \lesssim \xi_c$ . On the other hand, for  $\lambda > \lambda_*$ , all sites on the same percolation cluster are strongly correlated in space, implying  $\xi_{\perp} \gtrsim \xi_c$ . We therefore conclude

$$\xi_{\perp} \approx \xi_c, \quad (14)$$

and the correlation length exponent  $\nu_{\perp}$  is also identical to its lattice percolation counterpart  $\nu_c$ .

We now turn to the dynamics of the nonequilibrium transition across the percolation threshold. In order to find the time evolution of the total density of active sites (starting from a completely active lattice), we sum over all percolation clusters by combining the cluster size distribution (6) with the single-cluster time evolution (9). The total density is thus given by

$$\begin{aligned} \rho(t, \Delta) &= \int ds s n_s(\Delta) \rho_s(t) \\ &\sim \int ds s n_s(\Delta) \exp[-t/t_s(s)] \end{aligned} \quad (15)$$

In the following, we evaluate this integral at the transition as well as in the active and inactive phases.

Right at the percolation threshold, the scaling function in the cluster size distribution (6) is a constant,  $f(0)$ , and (15) simplifies to

$$\rho(t, 0) \sim \int ds s^{1-\tau_c} \exp[-(t/t_0 e^{As})]. \quad (16)$$

To estimate this integral, we note that only sufficiently large clusters, with a minimum size of  $s_{\min}(t) = A^{-1} \ln(t/t_0)$ , contribute to the total density at time  $t$ ,

$$\rho(t, 0) \sim \int_{s_{\min}}^{\infty} ds s^{1-\tau_c} \sim s_{\min}^{2-\tau_c}. \quad (17)$$

The leading long-time dependence of the total density right at the percolation threshold thus takes the unusual logarithmic form

$$\rho(t, 0) \sim [\ln(t/t_0)]^{-\bar{\delta}}, \quad (18)$$

again reflecting the activated dynamical scaling, with the critical exponent given by  $\bar{\delta} = \tau_c - 2 = \beta_c/(\nu_c D_f)$ .

In the disconnected, inactive phase ( $p > p_c$ ) we need to use expression (7) for the scaling function of the cluster size distribution. The resulting integral for the time evolution of the density reads

$$\rho(t, \Delta) \sim \int ds s^{1-\tau_c} \exp[-B_1 s \Delta^{1/\sigma_c} - (t/t_0 e^{As})]. \quad (19)$$

For long times, the leading behavior of the integral can be calculated using the saddle-point method. Minimizing the exponent of the integrand shows that the main contribution at time  $t$  to the integral (19) comes from clusters of size  $s_0 = -A^{-1} \ln[B_1 \Delta^{1/\sigma_c} t_0 / (At)]$ . Inserting this into the integrand results in a power-law density decay

$$\rho(t, \Delta) \sim (t/t_0)^{-d/z'} \quad (p > p_c). \quad (20)$$

The nonuniversal exponent  $z'$  is given by  $z' = (Ad/B_1) \Delta^{-1/\sigma_c} \sim \xi_{\perp}^{D_f}$ , i.e., it diverges at the critical point  $p = p_c$ .

In the percolating, active phase ( $p < p_c$ ), the infinite percolation cluster contributes a nonzero steady state

density  $\rho_{\text{st}}(\Delta)$  given by (13). However, the long-time approach of the density towards this value is determined by the slow decay of the metastable states of large finite-size percolation clusters. To estimate their contribution, we must use the expression (8) for the scaling function of the cluster size distribution. The resulting integral now reads

$$\begin{aligned} \rho(t, \Delta) - \rho_{\text{st}}(\Delta) &\sim \int ds s^{1-\tau_c} \exp \left[ -(B_2 s |\Delta|^{1/\sigma_c})^{1-1/d} \right. \\ &\quad \left. - (t/t_0 e^{As}) \right]. \end{aligned} \quad (21)$$

We again apply the saddle-point method to find the leading low-time behavior of this integral. Minimizing the exponent shows the main contribution coming from clusters of size  $s_0 = -A^{-1} \ln[B_2 |\Delta|^{1/\sigma_c} (d-1)/(Atd)]$ . By inserting this into the integrand, we find a nonexponential density decay of the form

$$\rho(t, \Delta) - \rho_{\text{st}}(\Delta) \sim e^{-[(d/z'') \ln(t/t_0)]^{1-1/d}} \quad (p < p_c). \quad (22)$$

Here,  $z'' = (Ad/B_2) |\Delta|^{-1/\sigma_c} \sim \xi_{\perp}^{D_f}$  is another nonuniversal exponent which diverges at the critical point.

The slow nonexponential relaxation of the total density on both sides of the actual transition as given in (20) and (22) is characteristic of a Griffiths phase [35] in the contact process [36]. It is brought about by the competition between the exponentially decreasing probability for finding a large percolation cluster off criticality and the exponentially increasing lifetime of such a cluster. Note that time  $t$  and spatial correlation length  $\xi_{\perp}$  enter the off-critical decay laws (20) and (22) in terms of the combination  $\ln(t/t_0)/\xi_{\perp}^{D_f}$  again reflecting the activated character of the dynamical scaling.

### C. Spreading from a single seed

After having discussed the time evolution of the density starting from a completely infected lattice, we now consider the survival probability  $P_s(t)$  for runs starting from a single random seed site. To estimate  $P_s(t)$ , we note that the probability of a random seed site to belong to a cluster of size  $s$  is given by  $s n_s(\Delta)$ . The activity of the contact process is confined to this seed cluster. Following the arguments leading to (9), the probability that this cluster survives is proportional to  $\exp(-t/t_s)$ . The average survival probability at time  $t$  can thus be written as a sum over all possible seed clusters,

$$P_s(t, \Delta) \sim \int ds s n_s(\Delta) \exp[-t/t_s(s)]. \quad (23)$$

This is exactly the same integral as the one governing the density decay (15). We conclude that the time dependence of the survival probability for runs starting from a single seed is identical to the time evolution of the density when starting from a fully infected lattice, as is expected

for the contact process under very general conditions (see, e.g., Ref. [5]).

To determine the (average) total number  $N(t)$  of active sites in a cloud spreading from a single seed, we observe that a supercritical cloud initially grows ballistically. This means its radius grows linearly with time, and the number of active sites follows a power law. This ballistic growth stops when the number of active sites is of the order of the cluster size  $s$ . After that, the number of active sites stays approximately constant. The number  $N_s(t)$  of active sites on a percolation cluster of size  $s$  is thus given by

$$N_s(t) \sim \begin{cases} (t/t_0)^{D_f} & (t < t_i(s)) \\ s & (t > t_i(s)) \end{cases} \quad (24)$$

where  $t_i(s) \sim R_s(s) \sim t_0 s^{1/D_f}$  is the saturation time of this cluster. Note that  $N_s$  decays to zero only after the much longer cluster lifetime  $t_s(s) = t_0 \exp[A(\lambda)s]$  given in (10).

We now average over all possible positions of the seed site as in (23). This yields

$$N(t, \Delta) \sim \int_{s_{\min}}^{\infty} ds s n_s(\Delta) N_s(t) \quad (25)$$

with  $s_{\min} \sim A^{-1} \ln(t/t_0)$ . At criticality, this integral is easily evaluated, giving

$$N(t, 0) \sim t^{D_f(3-\tau_c)} = t^{\gamma_c/\nu_c}. \quad (26)$$

The lower bound of the integral (i.e., the logarithmically slow long-time decay of the clusters) produces a sub-leading correction only. Consequently, we arrive at the somewhat surprising conclusion that the initial spreading follows a power-law and is thus much faster than the long-time density decay. In contrast, at the infinite-randomness critical point governing the generic ( $p < p_c$ ) transition, both the initial spreading and the long-time decay follow logarithmic laws [26, 27, 28, 29]. Note that a similar situation occurs at the percolation quantum phase transition in the diluted transverse-field Ising model [13] where the temperature-dependence of the correlation length does not follow the naively expected logarithmic law.

#### D. External source field

In this subsection we discuss the effects of spontaneous activity creation on our nonequilibrium phase transition. Specifically, in addition to healing and infection, we now consider a third process by which an inactive site can spontaneously turn into an active site at rate  $h$ . This rate plays the role of an external ‘‘source field’’ conjugate to the order parameter.

To find the steady state density in the presence of such a source field, we first consider a single percolation cluster. As before, we are interested in the supercritical regime  $\lambda > \lambda_*$ . At any given time  $t$ , a cluster of size  $s$  will be active (on average), if at least one

of the  $s$  sites has spontaneously become active within one lifetime  $t_s(s) = t_0 e^{As}$  before  $t$ , i.e., in the interval  $[t - t_s(s), t]$ . For a small external field  $h$ , the average number of active sites created on a cluster of size  $s$  is  $M_s(h) = h s t_s(s) = h s t_0 e^{As}$ . This linear response expression is valid as long as  $M_s \ll s$ . The probability  $w_s(h)$  for a cluster of size  $s$  to be active in the steady state is thus given by

$$w_s(h) \approx \begin{cases} M_s(h) & (M_s(h) < 1) \\ 1 & (M_s(h) > 1) \end{cases}. \quad (27)$$

Turning to the full lattice, the total steady state density is obtained by summing over all clusters

$$\rho_{\text{st}}(h, \Delta) \sim \int ds s n_s(\Delta) \min[1, M_s(h)]. \quad (28)$$

This integral can be evaluated along the same lines as the corresponding integral (15) for the time-evolution of the zero-field density. For small fields  $h$ , we obtain

$$\rho_{\text{st}}(h, 0) \sim [\ln(h_0/h)]^{-\delta} \quad (p = p_c), \quad (29)$$

$$\rho_{\text{st}}(h, \Delta) \sim (h/h_0)^{d/z'} \quad (p > p_c), \quad (30)$$

$$\delta\rho_{\text{st}}(h, \Delta) \sim e^{[(d/z'') \ln(h/h_0)]^{1-1/d}} \quad (p < p_c), \quad (31)$$

where  $\delta\rho_{\text{st}}(h, \Delta) = \rho_{\text{st}}(h, \Delta) - \rho_{\text{st}}(0, \Delta)$  is the excess density due to the field in the active phase and  $h_0 = 1/t_0$ . At criticality,  $p = p_c$ , the relation between density  $\rho_{\text{st}}$  and field  $h$  is logarithmic because the field represents a rate (inverse time) and the dynamical scaling is activated. Off criticality, we find strong Griffiths singularities analogous to those in the time-dependence of the density. The exponents  $z'$  and  $z''$  take the same values as calculated after eqs. (20) and (22), respectively.

#### E. Scaling theory

In Sections IV B and IV D, we have determined the critical behavior of the density of active sites by explicitly averaging the single cluster dynamics over all percolation clusters. The same results can also be obtained from writing down a general scaling theory of the density for the case of activated dynamical scaling [28, 29].

According to (13), in the active phase, the density is proportional to the number of sites in the infinite percolation cluster. Its scale dimension must therefore be identical to the scale dimension of  $P_\infty$  which is  $\beta_c/\nu_c$ . Time must enter the theory via the scaling combination  $\ln(t/t_0)b^\psi$  with the tunneling exponent given by  $\psi = D_f$  and  $b$  an arbitrary length scale factor. This scaling combination reflects the activated dynamical scaling, i.e., the exponential relation (12) between length and time scales. Finally, the source field  $h$ , being a rate, scales like inverse time. This leads to the following scaling theory of the density,

$$\begin{aligned} \rho[\Delta, \ln(t/t_0), \ln(h_0/h)] &= \\ &= b^{\beta_c/\nu_c} \rho[\Delta b^{-1/\nu_c}, \ln(t/t_0)b^\psi, \ln(h_0/h)b^\psi] \end{aligned} \quad (32)$$

This scaling theory is compatible with all our explicit results which can be rederived by setting the arbitrary scale factor  $b$  to the appropriate values.

## V. GENERALITY OF THE ACTIVATED SCALING SCENARIO

In Section IV, we have developed a theory for the nonequilibrium phase transition of the simple contact process across the lattice percolation threshold and found it to be characterized by unconventional activated dynamical scaling. In the present section, we investigate how general this exotic behavior is for absorbing state transitions by considering the generalized contact process with several absorbing states.

This is a particularly interesting question because the generic transitions ( $p < p_c$ ) of the diluted simple and generalized contact processes appear to behave differently. The generic transition in the simple contact process has been shown to be of infinite-randomness type with activated dynamical scaling using both a strong-disorder renormalization group [26, 27] and Monte-Carlo simulations [28, 29]. In contrast, the strong-disorder renormalization group treatment of the disordered generalized contact process [27] suggests more conventional behavior, even though the ultimate fate of the transition could not be determined.

To address the same question for our transition across the lattice percolation threshold, we note that any difference between the simple and the generalized contact processes must stem from the single-cluster dynamics because the underlying lattice is identical. In the following we therefore first give heuristic arguments for the single-cluster dynamics of the supercritical generalized contact process and then verify them by Monte-Carlo simulations.

If the percolation cluster is locally in the active phase ( $\lambda > \lambda_*$ ), the density time evolution, starting from a fully active lattice, proceeds in two stages, analogously to the simple contact process. There is a rapid initial decay to a metastable state with a nonzero density of active sites and finite-size islands of each of the inactive phases (see Fig. 5). For this metastable state to decay into one of the  $n$  absorbing configurations, all sites must go into *the same* inactive state which requires a rare large density fluctuation. Let us assume for definiteness that the decay is into the  $I_1$  state. The main difference to the simple contact process considered in Sec. IV A is that sites that are in inactive states  $I_2 \dots I_n$  cannot directly decay into  $I_1$ . This means, each of the inactive islands in states  $I_2 \dots I_n$  first needs to be “eaten” by the active regions before the entire cluster can decay into the  $I_1$  state. This can only happen via infection from the boundary of the active island and is thus a slow process. However, since the characteristic size of the inactive islands in the metastable state is finite (it is given by the connected density correlation length  $\xi_s^c$  on the cluster), this process happens with a nonzero

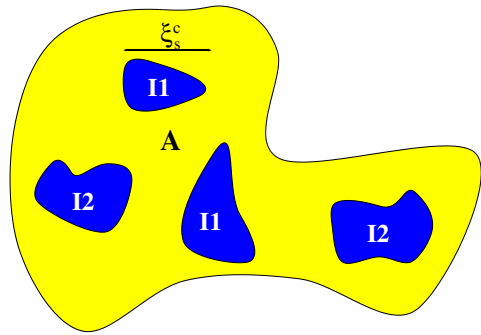


FIG. 5: (Color online:) Schematic of the metastable state of the supercritical generalized contact process with two inactive states on a single percolation cluster.  $A$  denotes the active state, and  $I_1$  and  $I_2$  are the inactive states.  $\xi_s^c$  is the connected correlation length of the density fluctuations *on* the cluster.

rate that is independent of the size  $s$  of the underlying percolation cluster (for sufficiently large  $s$ ).

The decay of the metastable state into one of the absorbing states is therefore brought about by the rare collective decay of a large number of *independent* correlation volumes just as in the simple contact process. As a result, the lifetime  $t_s(s)$  depends exponentially on the number of involved correlation volumes, i.e., it depends exponentially on the cluster size  $s$ . We thus find that the long-time density decay of the generalized contact process on a single large percolation cluster is governed by the same equations (9) and (10) as the decay of the simple contact process.

To verify these phenomenological arguments, we have performed large-scale Monte-Carlo simulations of the generalized contact process with two and three absorbing states on clean and disordered one-dimensional and two-dimensional lattices. In all cases, we have first performed bulk simulations (spreading from a single seed) to find the bulk critical point. An example is shown in Fig. 6, details of the bulk critical behavior will be reported elsewhere.

After having determined the critical point, if any, we have selected several parameter sets in the bulk active phase and studied the long-time density decay of the generalized contact process on finite size clusters. As expected, the decay proceeds via the two stages discussed above. As in Sec. IV A, we extract the lifetime  $t_s$  from the slow exponential long-time part of the decay. Two characteristic sets of results are shown in Fig. 7. The figure confirms that the lifetime of the generalized contact process on a finite-size cluster depends exponentially on the number of sites in the cluster, as given in (10). We have obtained analogous results for all cases investigated, verifying the phenomenological theory given above.

Because the long-time dynamics of the generalized contact process on a single supercritical cluster follows the same behavior (9) and (10) as that of the simple contact process, we conclude that its nonequilibrium transition across the percolation threshold will also be governed by

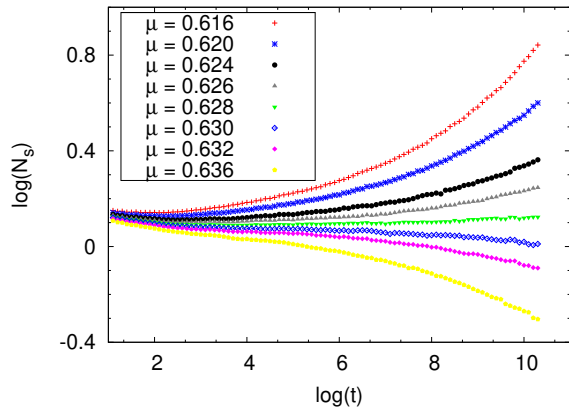


FIG. 6: (Color online:) Bulk phase transition of the generalized contact process with two absorbing states in  $d = 1$  measured via spreading from a single seed: Number  $N$  of active sites vs. time  $t$  for different healing rates  $\mu$ . The infection and boundary activation rates are fixed,  $\lambda = \sigma = 1$ , and the data are averages over  $10^6$  runs. The critical point appears to be close to  $\mu = 0.628$  in agreement with [20].

the theory developed on Sec. IV. In other words, the lattice percolation transitions of the simple and generalized contact processes belong to the same universality class, irrespective of the number  $n$  of absorbing states.

## VI. CONCLUSIONS

In this final section of the paper, we first summarize our results, discuss their generality, and relate them to the behavior of certain quantum phase transitions on diluted lattices. We then compare the recently found infinite-randomness critical point at the generic transition ( $p < p_c$ ) to the behavior at our lattice percolation transition. Finally, we relate our findings to a general classification of phase transitions with quenched spatial disorder [37].

To summarize, we have investigated absorbing state phase transitions on randomly diluted lattices, taking the simple and generalized contact processes as examples. We have focused on the nonequilibrium phase transition across the lattice percolation threshold and shown that it can be understood by combining the time evolution of the supercritical nonequilibrium process on a finite-size cluster with results from classical lattice percolation theory. The interplay between geometric criticality and dynamic fluctuations at this transition leads to a novel universality class. It is characterized by ultraslow activated (i.e., exponential) rather than power-law dynamical scaling and accompanied by a nonexponential decay in the Griffiths regions. All critical exponents of the nonequilibrium phase transition can be expressed in terms of the classical lattice percolation exponents. Their values are known exactly in two space dimensions and with good numerical accuracy in three space dimensions; they are

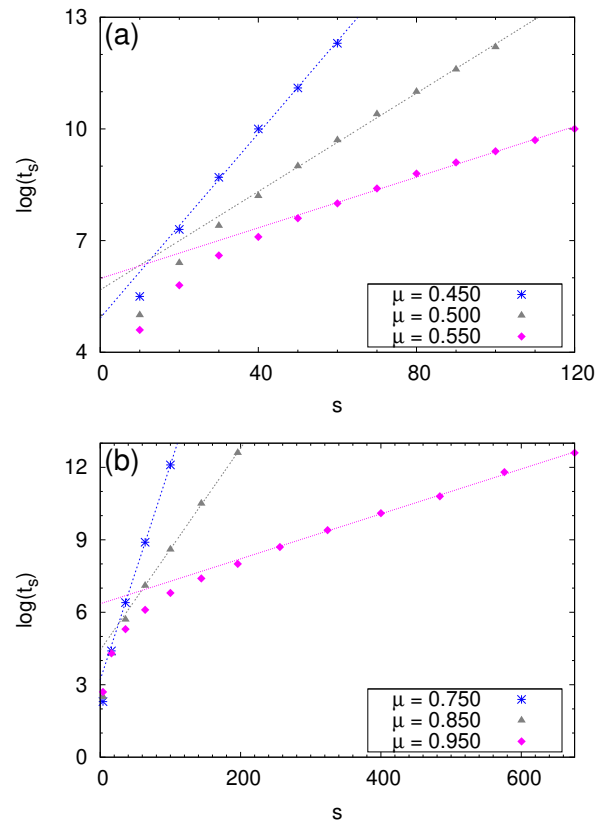


FIG. 7: (Color online:) Lifetime  $t_s$  as a function of cluster size  $s$  for the generalized contact process with two inactive states at different values of the healing rate  $\mu$ . The infection and boundary activation rates are fixed,  $\lambda = \sigma = 1$ , and the data are averages over  $10^6$  runs. (a)  $d = 1$  where the bulk system has a transition, see Fig. 6. (b)  $d = 2$ , where we do not find a bulk transition because the system is always active [32]. The dashed lines are fits of the large- $s$  behaviors to the exponential law (10).

TABLE I: Critical exponents of the nonequilibrium phase transition across the percolation threshold in two and three space dimensions.

Exponent	$d = 2$	$d = 3$
$\beta = \beta_c$	5/36	0.417
$\nu = \nu_c$	4/3	0.875
$\psi = D_f = d - \beta_c/\nu_c$	91/48	2.523
$\bar{\delta} = \beta_c/(\nu_c D_f)$	5/91	0.188

summarized in Table I. Thus, our transition in  $d = 2$  provides one of the few examples of a nonequilibrium phase transition with exactly known critical exponents.

The logarithmically slow dynamics (18), (29) at criticality together with the small value of the exponent  $\bar{\delta}$  make a numerical verification of our theory by simulations of the full diluted lattice a very costly proposition. The results of recent Monte-Carlo simulations in two di-

mensions [29] at  $p = p_c$  are compatible with our theory but not yet sufficient to be considered a quantitative verification. This remains a task for the future.

The unconventional critical behavior of our nonequilibrium phase transition at  $p = p_c$  is the direct result of combining the power-law spectrum (6) of cluster sizes with the exponential relation (12) between length and time scales. We therefore expect other equilibrium or nonequilibrium systems that share these two characteristics to display similar critical behavior at the lattice percolation transition. One prototypical example is the transverse-field Ising model on a diluted lattice. In this system, the quantum-mechanical energy gap (which represents an inverse time) of a cluster decreases exponentially with the cluster size. Consequently, the critical behavior of the diluted transverse-field Ising model across the lattice percolation threshold is very similar to the one found in this paper [13]. Other candidates are magnetic quantum phase transitions in metallic systems or certain superconductor-metal quantum phase transitions [38, 39, 40, 41], even though a pure percolation scenario may be hard to realize in metallic systems.

Our work has focused on the nonequilibrium phase transition across the lattice percolation threshold. It is instructive to compare its critical behavior to that of the generic transition occurring for  $p < p_c$  (see Fig. 1). Hooyberghs et al. [26, 27] applied a strong disorder renormalization group to the one-dimensional disordered contact process. They found an exotic infinite-randomness critical point in the universality class of the random-transverse field Ising model. The same analogy is expected to hold in two space dimensions. Recently, these predictions were confirmed by large scale Monte-Carlo simulations [28, 29]. Our nonequilibrium transition across the lattice percolation threshold shares some characteristics with these infinite-randomness critical points, in particular, the activated dynamical scaling which leads to a logarithmically slow density decay at criticality.

However, the generic and percolation transitions are in different universality classes with different critical exponent values. Moreover, the initial spreading from a single seed is qualitatively different (logarithmically slow at the generic infinite-randomness critical point but of power-law type at our percolation transition). Finally, at the percolation transition the simple and generalized contact processes are in the same universality class while this

does not seem to be the case for the generic transition [27].

The results of this paper are in agreement with a recent general classification of phase transitions with quenched spatial disorder and short-range interactions [37, 38]. It is based on the effective dimensionality  $d_{\text{eff}}$  of the droplets or clusters. Three classes need to be distinguished: (a) If the clusters are below the lower critical dimension of the problem,  $d_{\text{eff}} < d_c^-$ , the critical behavior is conventional (power-law scaling and exponentially weak Griffiths effects). This is the case for most classical equilibrium transitions. (b) If  $d_{\text{eff}} = d_c^-$ , the dynamical scaling is activated and accompanied by strong Griffiths effects. This case is realized at the nonequilibrium transition considered here as well as the generic transition of the disordered contact process. It also applies to various quantum phase transitions [13, 39, 42]. (c) If  $d_{\text{eff}} > d_c^-$ , a single supercritical cluster can undergo the phase transition independently of the bulk system. This leads to the smearing of the global phase transition; it occurs, e.g., in dissipative quantum magnets [43, 44] or in the contact process with extended defects [45].

In conclusion, our work demonstrates that absorbing state transitions on percolating lattices display unusual behavior. Interestingly, experimental verifications of the theoretically predicted critical behavior at (clean) absorbing state transitions are extremely rare [46]. For instance, to the best of our knowledge, the only complete verification of directed percolation scaling was found very recently in the transition between two turbulent states in a liquid crystal [47]. Our theory suggests that unconventional disorder effects may be responsible for the surprising absence of directed percolation scaling in at least some of the experiments.

## Acknowledgements

This work has been supported in part by the NSF under grant no. DMR-0339147, by Research Corporation, and by the University of Missouri Research Board. We gratefully acknowledge discussions with J. Hoyos as well the hospitality of the Max-Planck-Institute for Physics of Complex Systems during part of this research.

- 
- [1] T. M. Liggett, *Interacting particle systems* (Springer, Berlin, 1985).
  - [2] V. P. Zhdanov and B. Kasemo, *Surface Science Reports* **20**, 111 (1994).
  - [3] B. Schmittmann and R. K. P. Zia, in *Phase Transitions and Critical Phenomena*, edited by C. Domb and J. L. Lebowitz (Academic, New York, 1995), vol. 17, p. 1.
  - [4] J. Marro and R. Dickman, *Nonequilibrium Phase Transitions in Lattice Models* (Cambridge University Press, Cambridge, 1999).
  - [5] H. Hinrichsen, *Adv. Phys.* **49**, 815 (2000).
  - [6] G. Odor, *Rev. Mod. Phys.* **76**, 663 (2004).
  - [7] S. Lübeck, *Int. J. Mod. Phys. B* **18**, 3977 (2004).
  - [8] U. C. Täuber, M. Howard, and B. P. Vollmayr-Lee, *J. Phys. A* **38**, R79 (2005).
  - [9] D. Stauffer and A. Aharony, *Introduction to Percolation Theory* (CRC Press, Boca Raton, 1991).
  - [10] T. K. Bergstresser, *J. Phys. C* **10**, 3381 (1977).

- [11] M. J. Stephen and G. S. Grest, Phys. Rev. Lett. **38**, 567 (1977).
- [12] Y. Gefen, B. B. Mandelbrot, and A. Aharony, Phys. Rev. Lett. **45**, 855 (1980).
- [13] T. Senthil and S. Sachdev, Phys. Rev. Lett. **77**, 5292 (1996).
- [14] A. W. Sandvik, Phys. Rev. Lett. **89**, 177201 (2002).
- [15] L. Wang and A. W. Sandvik, Phys. Rev. Lett. **97**, 117204 (2006).
- [16] T. Vojta and J. Schmalian, Phys. Rev. Lett. **95**, 237206 (2005).
- [17] P. Grassberger and A. de la Torre, Ann. Phys. (NY) **122**, 373 (1979).
- [18] H. K. Janssen, Z. Phys. B **42**, 151 (1981).
- [19] P. Grassberger, Z. Phys. B **47**, 365 (1982).
- [20] H. Hinrichsen, Phys. Rev. E **55**, 219 (1997).
- [21] T. E. Harris, Ann. Prob. **2**, 969 (1974).
- [22] W. Kinzel, Z. Phys. B **58**, 229 (1985).
- [23] A. J. Noest, Phys. Rev. Lett. **57**, 90 (1986).
- [24] A. G. Moreira and R. Dickman, Phys. Rev. E **54**, R3090 (1996).
- [25] H. K. Janssen, Phys. Rev. E **55**, 6253 (1997).
- [26] J. Hooyberghs, F. Igloi, and C. Vanderzande, Phys. Rev. Lett. **90**, 100601 (2003).
- [27] J. Hooyberghs, F. Igloi, and C. Vanderzande, Phys. Rev. E **69**, 066140 (2004).
- [28] T. Vojta and M. Dickison, Phys. Rev. E **72**, 036126 (2005).
- [29] T. Vojta, A. Farquhar, and J. Mast, Phys. Rev. E **79**, 011111 (2009).
- [30] T. Vojta and M. Y. Lee, Phys. Rev. Lett. **96**, 035701 (2006).
- [31] J. Hooyberghs, E. Carlon, and C. Vanderzande, Phys. Rev. E **64**, 036124 (2001).
- [32] For  $d = 2, n = 2$ , Hinrichsen [20] finds a mean-field transition while our own simulations suggest that the system always active. Since this difference is of no importance for the present paper, it will be addressed elsewhere.
- [33] We define  $p$  as the fraction of sites removed rather than the fraction of sites present.
- [34] R. Dickman, Phys. Rev. E **60**, R2441 (1999).
- [35] R. B. Griffiths, Phys. Rev. Lett. **23**, 17 (1969).
- [36] A. J. Noest, Phys. Rev. B **38**, 2715 (1988).
- [37] T. Vojta, J. Phys. A **39**, R143 (2006).
- [38] T. Vojta and J. Schmalian, Phys. Rev. B **72**, 045438 (2005).
- [39] J. A. Hoyos, C. Kotabage, and T. Vojta, Phys. Rev. Lett. **99**, 230601 (2007).
- [40] A. Del Maestro, B. Rosenow, M. Müller, and S. Sachdev, Phys. Rev. Lett. **101**, 035701 (2008).
- [41] T. Vojta, C. Kotabage, and J. A. Hoyos, Phys. Rev. B **79**, 024401 (2009).
- [42] D. S. Fisher, Phys. Rev. Lett. **69**, 534 (1992).
- [43] T. Vojta, Phys. Rev. Lett. **90**, 107202 (2003).
- [44] J. A. Hoyos and T. Vojta, Phys. Rev. Lett. **100**, 240601 (2008).
- [45] T. Vojta, Phys. Rev. E **70**, 026108 (2004).
- [46] H. Hinrichsen, Braz. J. Phys. **30**, 69 (2000).
- [47] K. A. Takeuchi, M. Kuroda, H. Chate, and M. Sano, Phys. Rev. Lett. **99**, 234503 (2007).